FATIGUE MECHANISMS IN SHORT GLASS FIBRE REINFORCED THERMOPLASTIC: *IN SITU* X-RAY MICROTOMOGRAPHY OBSERVATIONS AND MICROSTRUCTURE MODELLING

H. Rolland[1], N. Saintier[1], C. Mareau[2], G. Robert[3]

[1]I2M, DuMAS, Arts et Metiers ParisTech, Esplanade des Arts et Metiers - 33400 Talence, France
[2]LAMPA, PMD, Arts et Metiers ParisTech, Boulevard du Ronceray - 49035 Angers, France
[3]Solvay Engineering Plastics, Avenue Ramboz - BP 64 - 69192 Saint Fons, France

Keywords: Fatigue, Reinforced polyamide, Damage mechanisms, X-ray microtomography,

Abstract
Short glass fibre reinforced thermoplastics are promising materials for weight reduction of structures thanks to their very good specific mechanical properties. The current challenge is to provide experimental data concerning damage mechanisms and their kinetics in order to enhance micromechanical models for these materials with complex behaviour. The objective of this work is therefore to observe and explain damage mechanisms regarding spatial configuration of the microstructure. Fatigue tests have been running on reinforced polyamide specimens and interrupted at different levels of the estimated life. 3D pictures of the gage length of these specimens have been obtained by microtomography with high resolution ($0.65\mu m$). This data presents damage location at different stages of lifetime. Thus, debonding, matrix damage and fibre failure have been identified as the three damage mechanisms for these materials. The analysis of the evolution of the damage markers quantity, volume and aspect ratio inform about the kinetic for each mechanism during the material life.

1. Introduction

With increasing constraints of weight reduction of vehicles in industrial fields, mechanical properties are now considered regarding material density. This trend ranks the short glass fibre reinforced polyamide 6,6 among very promising materials, whence emerges the need to describe its intricate behaviour. This complexity mainly comes from the microstructure of the material: the injection process, perfectly suited for high productivity and complex shapes, induces heterogeneous distribution and orientation of fibres and complex matrix/fibre interactions [1, 2]. A first description of damage chronology has been made by Horst [3, 4] for fatigue loading from SEM surface observation. In order to evaluate spatial configuration of damage and chronology, the present work proposes an X-ray microtomography based study of 3D damage observation.

2. Experimental

2.1. X-ray Microtomography

X-ray computed microtomography is an observation technique based on the acquisition of X-ray radiographs obtained for different angular positions of the sample with respect to the beam. These sets of X-ray radiographs are put together to obtain the three dimensional distribution of the linear X-ray attenuation coefficient within the sample. This distribution forms a 3D image where the elementary unit is

Excerpt from ISBN 978-3-00-053387-7

called a voxel (*volumetric pixel*).

Experiments presented in this paper were performed on ID19 beamline at the European Synchrotron Radiation Facility (Grenoble, France). A pink X-ray beam was used in mode 16 bunches, with a photon energy of 19 keV. A PCO edge camera with a 2048 x 2048 pixel sensor received 6000 X-ray radiographs during a rotation of the specimen over 180°along vertical axis. This experimental set-up was optimized to obtain a voxel edge size of 0.65μm. The acquisition of a complete scan lasts about 7 minutes. This first set of experiment was completed by additional imaging on Psyche beamline at the Synchrotron Soleil (Saclay, France). For this set-up, the filtered X-ray beam (2 mrad mirror, 0.5 mm aluminum and 0.25 mm silver) had an energy of around 26 keV. The CMOS detector with a 6.5 micron pixels, was associated to a x10 objective, leading to a voxel edge size of 0.65μm. Specimen-sensor distance was 35 mm. 1500 projections were recorded per scan during a 180 degrees rotation of around 5 min, with 31 references pictures before and after scanning.

2.2. Specimen

The studied material is Technyl®A218V30, a commercial grade of polyamide 6,6 reinforced by 30wt% of short glass fibre supplied by Solvay Engineering Plastics-France. Water content for specimens of the study has been fixed at 50% of relative humidity (RH50). The injection process used to form rectangular plates induces an heterogeneous orientation of fibres in the thickness of the specimen, commonly designated as a core-shell-skin structure. In these specimens, the shell layer is the largest with a thickness of 1.4 mm with its fibres in the mould flow direction (MFD). The core is 300μm thick in the centre of the specimen, fibres being perpendicular to the MFD. The observed zone by tomography is a cube of 1.66 mm edge size, centered on the gage length of the specimen.

2.3. Procedure

The study has been designed to observe fatigue damage mechanisms. Fatigue tests have been run and interrupted at different levels of their estimated life. For a given life time, four observations have been made : a non-fatigued reference and three specimens interrupted at 50%, 75% and 95% of the estimated life. Fatigue tests were performed on a compact home made fatigue test machine completed by interrupted fatigue test on a BOSE fatigue machine. During the microtomography process, specimens were maintained under stress (limited to half maximal stress of the fatigue test) by a compact tensile machine in order to facilitate observation of damages in the material. This machine (presented in Fig. 1) has been especially designed for this experiment with X-ray microtomography. At the height of the specimen gage length, the machine part is a thin and homogeneous part of PMMA to minimize attenuation of the set-up. The displacement is controlled by a step motor and the load measured with a load cell.

3. Preliminary results on analysis of damage markers morphology

Series of tensile tests on this material had been observed with the same procedure in a previous work [5]. The analysis of this data allowed to distinguish three main damage mechanisms: fibre failure, matrix damage, damage at the fibre-matrix interface (including debonding and damage initiation at fibre ends). Each mechanism has been associated with damage markers geometric measurements as illustrated Fig. 2.

Excerpt from ISBN 978-3-00-053387-7

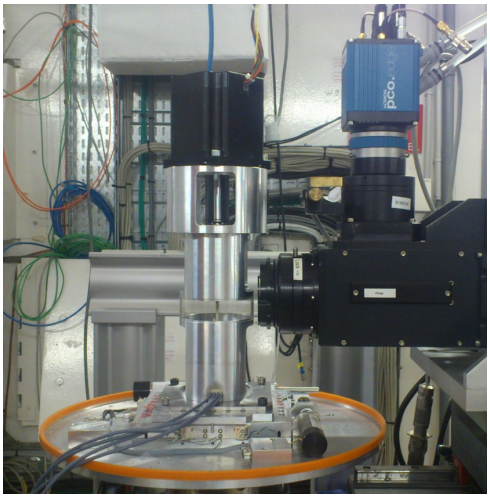

Figure 1. Experimental set-up on ID19 beamline - ESRF

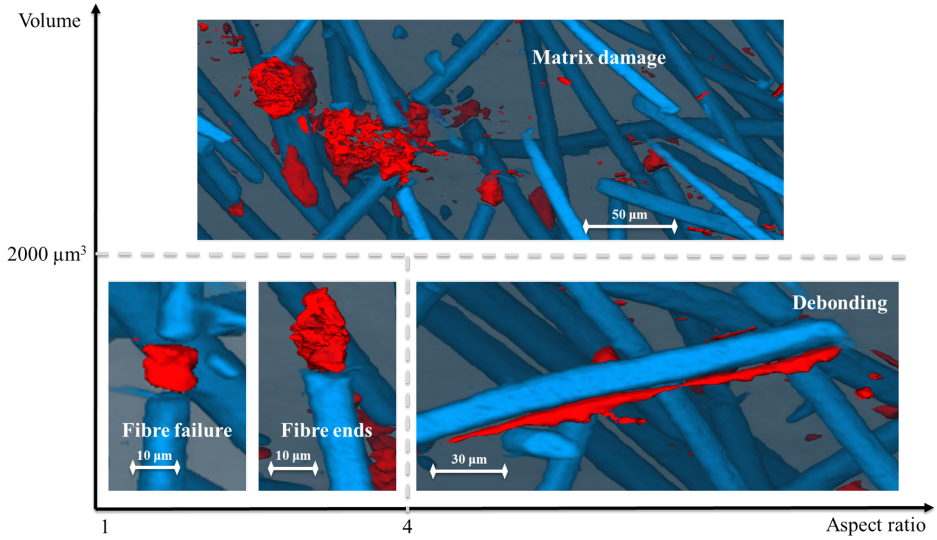

Figure 2. Quasi-static mechanisms classification based on geometrical aspects of damage markers [5]

Excerpt from ISBN 978-3-00-053387-7

4. Results and Discussion

4.1. Observed fatigue mechanisms

The observed mechanisms are slightly different between fatigue and quasi-static stresses. Indeed, if damage at the fibre-matrix interface (debonding and damage at fibre ends) and fibre failure are common damage mechanisms, there is no matrix cavity growth in fatigue. Moreover, micro-cavitation and cracks are detected in fatigued specimens. Fibre failure is widespread in the material. Systematic fibre crossing near any fibre failure has to be noticed, as shown in Fig. 3(a), suggesting important overstress is locally induced by the microstructure. Damage at fibre ends has been observed during both quasi-static and fatigue testing. Debonding is also observed among fatigue damage mechanisms (cf. Fig. 3(b)). It has been pointed out that this mechanism is not consistently initiated at fibre ends, contrary to usual description found in literature. Indeed, this phenomenon is activated by fibre crossing at the fibre-matrix interface.

Matrix micro-cavitation has been observed during fatigue testing, as shown in Fig. 3(c), and is probably activated by long-term stress. This phenomenon brings precious information about damage evolution of the matrix. Finally microcracks and cracks have been observed in fatigued specimens. These lengthy markers arise from short distance interactions between nearby damage markers. Their development seems to be highly dependant on the local microstructure orientation. Indeed, cracks orientation tends to be perpendicular to the macroscopic tensile direction, until they run into a fibre. There, depending on the closest damage marker, the crack can coalesce with this marker or can be stopped if the distance or the deviation is too important.

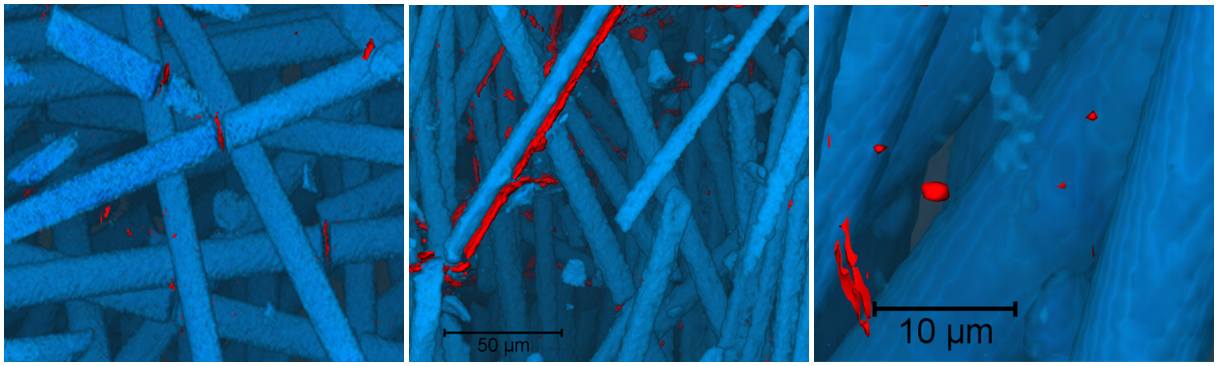

(a) Fibre failure (b) Debonding (c) Cavitation

Figure 3. RH50 - 45°specimen fatigued at 95% of its estimated life

4.2. Application to the observed volumes

Each damage markers were separated accordingly to their aspect ratio. Micro-cavitation, fibre ends damage and fibre failure, debonding and cracks are quantified by the number of counted damage markers. These quantities are presented in Fig. 4 for each identified mechanism. Micro-cavitation has been activated during fatigue testing. This matrix damage mechanism seems linked with long term stress application. The number of markers associated to micro-cavitation grows during the fatigue test as presented in Fig. 4(a).

Another damage mechanism in the matrix is the crack formation. Cracks appear where there is short distance interaction between pre-existing damage markers. This implies that microstructure plays an important role on the growth of these markers and therefore, on their number. In the case of shell in 0°oriented specimen, non-broken fibres constitute obstacles to crack growth and lead to an increase of the crack number, as seen in Fig. 4(b).

Concerning damage at the fibre-matrix interface, the number of markers corresponding to damage at fibre ends and fibre failures has a fast development for the three specimen orientations, shown in Fig. 4(c). Its quantity is more associated to the number of fibres than to their orientation. Indeed, the fibre geometry creates an overstress at fibre ends, where there is no sizing to improve mechanical properties of the interface. Debonding is also mostly activated by fibre crossing and not only by the difference between fibre orientation and tensile macroscopic direction. Fig. 4(d) shows that the evolution of the number of damage markers is important for 0°oriented specimens and subtle for 45°and 90°oriented specimens. This is probably due to the fact that distinction between debonding and crack is not totally perfect.

Excerpt from ISBN 978-3-00-053387-7

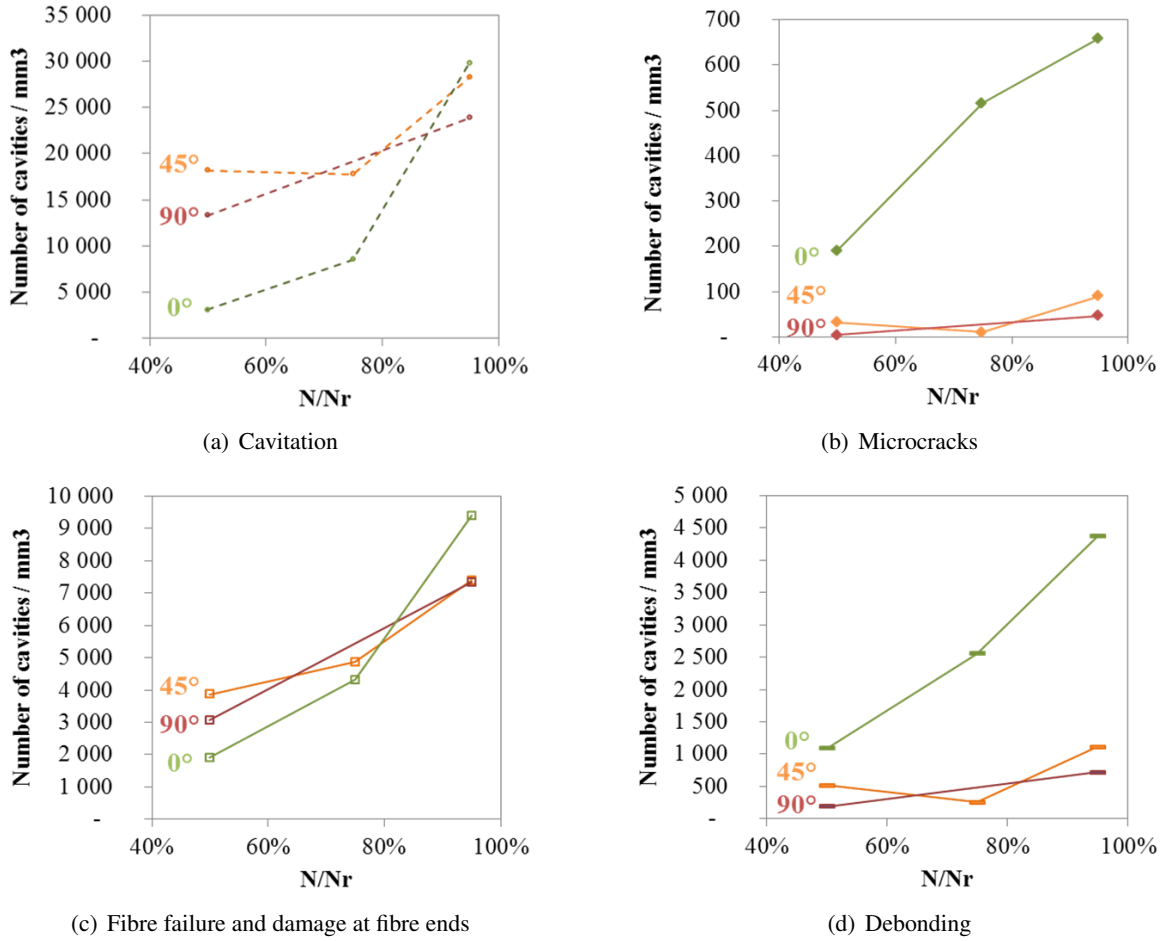

(a) Cavitation

(b) Microcracks

(c) Fibre failure and damage at fibre ends

(d) Debonding

Figure 4. Damage mechanism density evolution depending on specimen orientation

4.3. Damage mechanisms initiation and evaluated stress field

In order to identify the link between damage initiation and eventual overstress induced by the microstructure, a numerical computation has been led. This computation used a spectral method based on Moulinec and Suquets work [6]. An intensive use of the Fast Fourier Transform (FFT) algorithm is made to solve the integral equation associated with the heterogeneous problem. In contrast with the finite element method, the periodicity of both the microstructure and the boundary conditions is a necessary condition for the application of the spectral method FFT calculation. So, periodic microstructures have been generated with Digimat-FE with the objective to look alike observed microstructures in terms of volumetric fraction of fibres, fibres length distribution, fibres diameter and resulting orientation tensor. Then, three microstructures of around one hundred fibres have been obtained for each orientation (0°, 45°, 90°), as illustrated in Fig. 5. Each cubic microstructure has a 200μm edge size and is composed of 160 x 160 x 160 voxels. An elastic behaviour has been assigned to the glass fibres. An elasto-viscoplastic behaviour has been assigned to the matrix, based on direct identification from corresponding experimental results (RH0, RH50 and RH80) at different strain rates. Then a monotonic load is applied to the volume until a global strain of 5% to 10%, according to the chosen parameters (main orientation and conditioning). Results have been analysed to observe the different configurations of microstructure, their impact on the stress fields and to compare them to microstructures observed by X-ray microtomography, as presented in Fig. 6. Results show that overstressed zones do exist in the material and that these zones with higher stress intensities are related to local damage initiation.

Excerpt from ISBN 978-3-00-053387-7

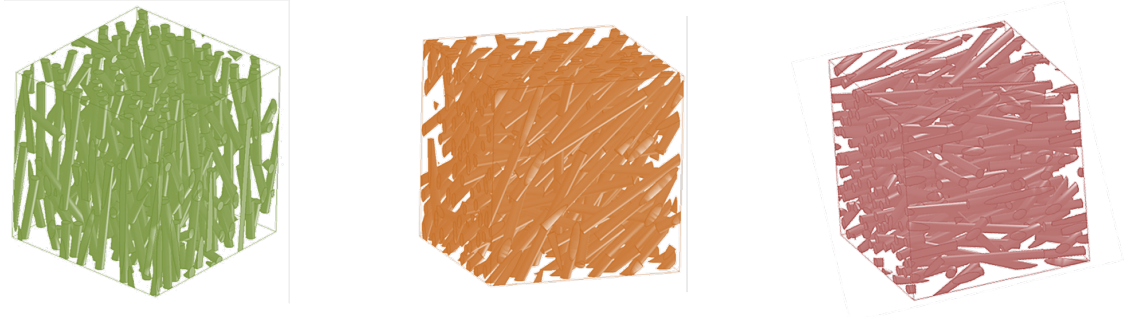

116 fibres (250 parts)
L_{mean} = 151,3 µm

Orientation tensor :		
0,85	0,014	0,022
	0,13	-0,0042
		0,023

(a) 0°oriented microstructure

111 fibres (276 parts)
L_{mean} = 156,0 µm

Orientation tensor :		
0,48	0,37	0,0099
	0,48	-0,0067
		0,045

(b) 45°oriented microstructure

115 fibres (260 parts)
L_{mean} = 149,3 µm

Orientation tensor :		
0,14	-0,051	-0,0009
	0,81	0,047
		0,053

(c) 90°oriented microstructure

Figure 5. Periodic microstructures generated

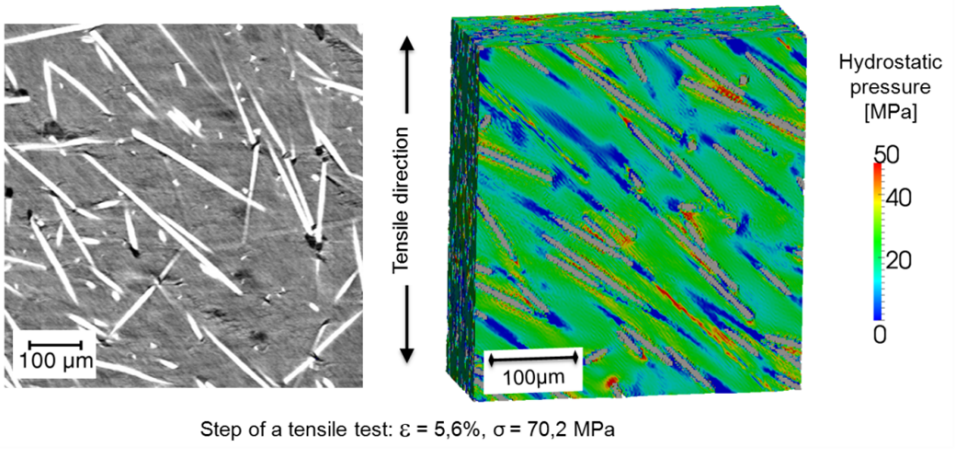

Figure 6. Comparison between microtomographic observations and results from numerical computation for a RH50 - 45°specimen

5. Conclusions

Damage mechanisms due to quasi-static and fatigue testing have been observed by X-ray microtomography. Observed damage markers are differentiated by their geometric aspects (length, volume and aspect ratio) and associated to each identified mechanism. This differentiation allows to quantify the development of these mechanisms at different levels of damage. Damage mechanisms kinetics are deduced for global observed volumes and bring precious information for physically based micro-mechanical modelling. At the micron scale, local microstructure singularities have been pointed out (fibre ends and fibres crossing). Computed stress fields indicate overstressed zones due to the microstructure and leading to damage initiation.

Excerpt from ISBN 978-3-00-053387-7

Acknowledgments

This work was performed in the context of the FUI project DURAFIP. The X-ray microtomography experiments performed at Soleil Synchrotron were financially supported by the synchrotron proposal n20150398.

References

[1] J.L. Thomason. The influence of fibre properties on the performance of glass-fibre-reinforced polyamide 6,6. *Composites Science and Technology*, 59:2315–2328, 1999.

[2] J.L. Thomason. The influence of fibre length, diameter and concentration on the modulus of glass fibre reinforced polyamide 6,6. *Composites: Part A*, 39:1732–1738, 2008.

[3] J. J. Horst and J. L. Spoormaker. Mechanisms of fatigue in short glass fiber reinforced polyamide 6. *Polymer Engineering & Science*, 36(22):2718–2726, 1996.

[4] J.J. Horst and J.L. Spoormaker. Fatigue fracture mechanisms and fractography of short-glassfibre-reinforced polyamide 6. *Journal of materials science*, 32(14):3641–3651, 1997.

[5] H. Rolland, N. Saintier, and G. Robert. Damage mechanisms in short glass fibre reinforced thermoplastic during in situ microtomography tensile tests. *Composites Part B*, 90:365–377, 2016.

[6] H. Moulinec and P. Suquet. A numerical method for computing the overall response of nonlinear composites with complex microstructure. *Compute*, 157:69–94, 1998.

Excerpt from ISBN 978-3-00-053387-7